6086–6099 *Nucleic Acids Research, 2011, Vol. 39, No. 14* *Published online 12 April 2011*
doi:10.1093/nar/gkr194

MicroRNA 130 family regulates the hypoxia response signal through the P-body protein DDX6

Ken Saito[1,2], Eisaku Kondo[2] and Masayuki Matsushita[1,*]

[1]Department of Molecular and Cellular Physiology, Graduate School of Medicine, University of the Ryukyus, 207 Uehara, Nishihara, Okinawa 903-0215 and [2]Division of Oncological Pathology, Aichi Cancer Center Research Institute, 1-1 Kanokoden, Chikusa-ku, Nagoya 464-8681, Japan

Received November 15, 2010; Revised March 16, 2011; Accepted March 17, 2011

ABSTRACT

The transcription factor HIF-1α (hypoxia inducible factor 1α) has an essential role in the maintenance of oxygen homeostasis in metazoans. HIF-1α expression and activity in the hypoxic response is regulated at the translation and post-translational levels. However, the mechanism and modulator of HIF-1α translation during hypoxia is not fully understood. We found that HIF-1α expression during hypoxia was upregulated by the microRNA 130 (miR-130) family. Levels of the miR-130 family are elevated under hypoxia, and their target is DDX6 mRNA, which is a component of the P-bodies. Furthermore, we found that a decrease of DDX6 expression by the miR-130 family enhanced the translation of HIF-1α in an internal ribosome entry site element-dependent manner. These results reveal a new HIF-1α translational mechanism and a role for P-bodies in hypoxic stress.

INTRODUCTION

Metazoans respond to hypoxia with adaptive changes in gene expression through the transcription factor HIF-1α (hypoxia inducible factor 1α) (1–3). HIF-1α is hydroxylated by prolyl hydroxylases (PHDs) of the 2-OG-Fe(II) dioxygenase family under normoxia, and then hydroxylated HIF-1α is degraded by a proteasome through interactions with the pVHL E3 ubiquitin ligase complex (4). However, oxygen-dependent hydroxylation of HIF is reduced in hypoxia, resulting in the stabilization, activation (4–6), and induction of gene expression such as glucose transporters and vascular endothelial growth factor (VEGF). In translational regulation, it has been suggested that activation of the PI3K-Akt-mTOR pathway and MAPK pathway induce the translation of HIF-1α in a 5′ cap-dependent manner under normoxia (7). Under hypoxic conditions, despite decreased global protein translation, HIF-1α synthesis is constitutively induced (8). Several studies have suggested that the mRNA-binding proteins PTB and HuR interact with the internal ribosome entry site (IRES) and facilitate the translation of HIF-1α (9,10). Moreover, overexpressed 4E-BP and eIF4G in cancer cells also enhance the translation of HIF-1α during hypoxia (11). However, the mechanism and modulator of HIF-1α translation during hypoxia have not been fully elucidated.

Recently, it was demonstrated that microRNAs (miRNAs) are involved in the translational regulation of mRNAs (12). miRNA genes are expressed as primary transcripts (pri-miRNA) that are finally processed to mature miRNAs via precursor miRNAs (pre-miRNA). The mature miRNAs (~22 nt non-coding RNAs) form partial base pairs, called seed matches, to target mRNAs at the 3′-untranslated region (3′UTR) of the target gene. However, plant miRNA–mRNA interactions, for example, have an imperfect seed match (13). It has been suggested that residues beyond the seed sequence play an important role in central pairing (14). Finally, the mature miRNAs guide the RNA-induced silencing complex (RISC) to the target mRNAs (15), and these components accumulate in the P-bodies, which are cytoplasmic foci containing translationally repressed mRNP complexes (16). Furthermore, it has been reported that mature miRNAs binding to the coding sequence induce cleavage of target mRNA in a manner similar to small interfering RNAs (17).

On the other hand, the translation of TNF-α mRNA is induced by the binding of the miRNA–Ago2–FXR1 complex to the TNF-α 3′UTR when mammalian cells are deprived of serum and the cell cycle is arrested (18). Interestingly, recent studies revealed that miR-122 in liver cells binds to the 5′UTR of the hepatitis C virus (HCV) genome and enhances HCV RNA levels (19,20). In addition, it has been suggested that CAT-1 mRNA is relieved from miR-122-mediated repression. The process involves HuR for release from P-bodies, and CAT-1 mRNA reenters the polysomes (21). These studies

*To whom correspondence should be addressed. Tel: +81 098 895 1106; Fax: +81 098 895 1402; Email: masayuki@med.u-ryukyu.ac.jp

indicate that miRNAs and ribonucleoproteins have both negative and positive regulatory functions in targeting mRNAs and RNA genomes (18–20,22).

In this study, we report that the miR-130 family targets DDX6 mRNA, which is a component of the P-bodies (23), and facilitates the translation of HIF-1α during hypoxia.

MATERIALS AND METHODS

Cell lines

The human kidney cell line HEK293 was obtained from the Health Science Research Resources Bank (Japan) and maintained in DMEM (Gibco) containing 10% FBS with penicillin-streptomycin (Gibco) at 37°C with 5% CO_2. Hypoxia was achieved in a hypoxic chamber (Wakenyaku) filled with 5% CO_2 and 0.1% O_2 balanced with N_2. Hippocampus neuronal cells were dissected from 18.5-day embryonic mice and dispersed by gentle pipetting in neurobasal medium (Gibco) and centrifuged at 1000 rpm for 5 min. Cells were plated on poly-L-lysine and laminin-coated dishes containing neurobasal medium and B27 (Gibco) with penicillin–streptomycin. Cells were cultured for 7–10 days at 37°C with 5% CO_2.

Plasmid construction

Human DDX6 cDNA (clone ID: 6163439, NCBI accession BC065007) was obtained from OPEN BIOSYSTEMS. DDX6 was amplified with primers by PCR using DDX6 cDNA as the template. The PCR products were cloned into the pcDNA3 vector (Invitrogen) in the HindIII and BamHI sites. To generate FLAG-DDX6, DDX6 ORF was cloned into pFLAG-CMV2 (Sigma) in the NotI and BamHI sites. The p3×FLAG-EGFP plasmid was generated by cloning the EGFP-coding region of the pEGFP-N1 vector (Clontech) into the p3×FLAG-myc-CMV-24 vector (Sigma) in the BamHI and NotI sites.

For the reporter plasmid containing the DDX6 3′UTR region, DDX6 3′UTR (800 bp) was amplified with primers by PCR using DDX6 cDNA as the template. The PCR products were cloned into the psiCHECK-2 vector (Promega) in the XhoI and NotI sites. DDX6 3′UTR mutagenesis was performed using the QuickChange kit (Stratagene). For the HIF-1α 3′UTR reporter plasmid, mouse HIF-1α cDNA (RIKEN FANTOM clone ID9330155D13, NM_010431) was obtained from DNAFORM, Japan. The HIF-1α 3′UTR (1200 bp) was amplified with primers by PCR. The PCR products were cloned into the psiCHECK-2 vector (Promega) in the XhoI and NotI sites.

For *in vitro* translation, HIF-1α IRES (259 bp) in the 5′UTR was amplified with primers by PCR using mouse HIF-1α cDNA as the template. The PCR products were cloned into the pBluescript II SK (-) vector (Stratagene) in the XhoI and BamHI sites. A portion of the HIF-1α coding region (437 bp) was generated by SalI and HindIII digestion of mouse HIF-1α cDNA. The fragments were inserted into the pBluescript II SK (-) vector. The nucleotide sequences of all constructs obtained by PCR were confirmed by DNA sequencing. The primers are shown in Supplementary Table S3.

Western blots

HEK293 cells, 4×10^5, were seeded in 35-mm dishes. After pre-miRNA transfection and hypoxia treatment, cells were lysed with 200 μl of 2 × SDS sample buffer (250 mM Tris–HCl pH 6.8, 4% SDS, 20% glycerol, 0.01% bromophenol blue) containing 10% β-ME, harvested and sonicated. After boiling for 2 min, proteins were subjected to SDS-polyacrylamide gels and blotted onto nitrocellulose membranes. Non-specific binding sites were blocked with 5% skimed milk powder in TBST (50 mM Tris–HCl pH 7.2, 140 mM NaCl, 0.05% Tween-20) for 1 h. HIF-1α antibody (1:1000), HIF-1β antibody (1:1000), DDX6 antibody (1:5000) and Actin antibody (1:10 000) were added and incubated overnight at 4°C. Afterward, nitrocellulose membranes were washed three times for 10 min with TBST. The membranes were then incubated with anti-mouse or anti-rabbit secondary antibodies conjugated with HRP (1:1000) for 1 h and washed three times for 10 min with TBST. Detection was followed by ECL (Bio-Rad) and visualized by a VersaDOC instrument (Bio-Rad).

RNA isolation and northern blots

HEK293 cells were seeded at a density of 2×10^6 cells/10 ml in 100-mm dishes. The next day, the medium was changed to fresh DMEM and then cells were treated with normoxic or hypoxic conditions for 48 h. RNA was extracted using Trizol (Invitrogen) according to the manufacturer's protocol. The RNA was quantified by absorbance at 260 nm, and 40 μg of total RNA was resolved by electrophoresis through a 15% TBE/urea gel (Invitrogen). After electrophoresis, the gel was stained with ethidium bromide and transferred to Hybond N^+ (GE Healthcare) in a semi-dry transfer system (Taitech) at 200 mA for 90 min. The RNA was fixed to the membrane by a UV crosslinker and pre-hybridized in 5 ml of PerfectHyb hybridization solution (Toyobo) for 60 min at 37°C. One microliter of DIG labeling locked nucleic acid probes (50 μM), miR-130a LNA and miR-130b LNA, were added to 5 ml of PerfectHyb hybridization solution. Hybridization was carried out at 25°C for 24 h. The membrane was washed three times for 5 min at 55°C with 2 × SSC/0.1% SDS, and incubated at room temperature for 1 h with anti-DIG-AP at a dilution of 1:10 000 in blocking buffer (Roche). Hybridization signal was detected using a CDP-star (Roche) and visualized by exposure to X-ray film. miR-130a and -130b locked nucleic acids probes (Thermo) are shown in Supplementary Table S4.

Quantitative real-time PCR

Total RNA (1 μg) was reverse-transcribed at 42°C for 15 min, 95°C for 2 min and 4°C with random 6-mer oligos and the ExScript RT reagent kit (Takara) in 20 μl of reaction solution. RT–PCR products were diluted 1:20. Diluted RT–PCR products (2 μl) were subjected to quantitative real-time PCR using a SYBR Premix Ex Taq kit

(Takara) in 20 μl of reaction solution. Quantitative real-time PCR and data analysis were performed with a Light Cycler 1.5 system (Roche). PCR was performed as follows: pre-denaturation at 95°C for 2 min, 50–60 cycles of denaturation at 95°C for 10 sec, annealing at 55°C for 20 s and extension at 72°C for 30 s. For the reverse-transcription of pre-miRNA, the RT-enzyme solution was added to the reaction solution after incubation at 95°C for 10 s, and then reverse-transcription was performed with random 6-mer oligos. Pri- and pre-miRNA levels in qRT–PCR were normalized by 5S rRNA.

For mature miRNA analysis, RT–PCR was performed as previously described (24). Total RNA was reverse-transcribed at 16°C for 30 min, 42°C for 30 min, 95°C for 2 min and 4°C with 1 μM of stem–loop RT primers and the ExScript RT reagent kit (Takara). Mature miR-130a and -130b RNA levels in qRT–PCR were normalized by 5S rRNA based on a standard curve using RT–PCR products from lin-4 synthetic miRNA. Primers are shown in Supplementary Table S3.

Reporter gene assay

HEK 293 cells were seeded in 24-well plates (Iwaki) at 5×10^4 cells/well. The cells were co-transfected using Lipofectamine LTX transfection reagent (Invitrogen) with 170 ng of firefly luciferase reporter plasmids and 80 ng of Renilla luciferase plasmid pGL4.74 (Promega). For the firefly luciferase reporter plasmid, pHRE-Luc (T. Imai and H. Okano, unpublished data) containing six copies of the hypoxia-response element from the transferrin promoter and pNFκB-Luc (BD Clontech) were used. Five hours after transfection of reporter plasmids, 10 nM of pre-miRNAs were transfected into the cells using the DharmaFECT1 transfection reagent (Dharmacon). At 48 h after transfection of pre-miRNAs, the cells were exposed to 0.1% O_2 or treated with 20 ng/ml TNF-α for 12 h. Cell extracts were prepared in Passive Lysis Buffer (Promega) and luciferase assays were done with a Dual-Luciferase assay kit (Promega) following the manufacturer's protocol. HRE luciferase and NF-κB luciferase values were divided by Renilla luciferase values to correct for variations in transfection efficiency. Luminescence was measured using a Centro XS3 LB 960 microplate luminescence reader (Berthold).

For the HIF-1α IRES reporter assay, we used pRF plasmid and pRhifF plasmid-containing mouse HIF-1α IRES between Rluc and Fluc, which were a kind gift from Dr J. Gregory Goodall (University of Adelaide, Australia) (7). HEK293 cells were transfected with 50 nM of pre-miRNAs or 50 nM of siRNAs. After 48 h, cells were transfected with either pRF (250 ng) or pRhifF (250 ng) for 24 h. IRES activities during normoxia were represented as the expression of firefly to Renilla luciferase. For the DDX6 3′UTR and HIF-1α 3′UTR reporter assay, HEK 293 cells were seeded in 24-well plates (Iwaki) at 1×10^5 cells/well. The cells were co-transfected using Lipofectamine 2000 transfection reagent (Invitrogen) with 50 ng of reporter plasmid and 25 nM of miRNAs. After 48 h, Renilla and firefly luciferase were measured.

IP of RNP complexes

HEK293 cells were seeded at a density of 1×10^6 cells/10 ml in 100-mm dishes. After 48 h, cells were washed with PBS and harvested using 500 μl of lysis buffer (10 mM HEPES pH 7.0, 100 mM KCl, 5 mM $MgCl_2$, 0.5% NP-40, 1 mM DTT) containing 100 U/ml RNase OUT (Invitrogen) and protease inhibitor cocktail (Roche). Cell lysates were centrifuged at 15 000 rpm for 30 min at 4°C. Supernatants were pre-incubated with protein G sepharose (GE Healthcare) containing 0.1% BSA at 4°C for 1 h, and the resin was removed by centrifugation. The supernatants (600 μg of protein) were incubated with anti-DDX6 antibody at 4°C overnight. A 50% suspension of protein G sepharose containing 0.1% BSA and including anti-DDX6 antibody was added to the supernatants and was incubated at 4°C for 1 h. The resin was washed five times with NT2 buffer (50 mM Tris–HCl pH 7.4, 150 mM NaCl, 1 mM $MgCl_2$ and 0.05% NP-40). Additionally, the resin was incubated with 100 μl NT2 buffer containing 20 U of DNase I for 15 min at 30°C, then washed twice with 0.5 ml NT2 buffer. For western blots, 2 × SDS sample buffer was added to the resin of protein–RNA complexes. DDX6 protein was detected by anti-DDX6 antibody. For RNA analysis, Trizol (Invitrogen) was added to the resin of protein–RNA complexes, and then RNA was isolated and dissolved in 10 μl of water. The RNA (50 ng) was reverse transcribed using random 6-mer oligos and the ExScript RT reagent kit (Takara). PCR for HIF-1α detection was performed as follows: pre-denaturation at 94°C for 2 min, 35 cycles of denaturation at 94°C for 30 s, annealing at 55°C for 30 s and extension at 72°C for 30 s. PCR for GAPDH was performed for 25 cycles. These primers are shown in Supplementary Table S3.

For the binding assay of HIF-1α IRES or CDS RNAs and FLAG-DDX6, RNAs were generated by linearizing the pBluescript II SK (-) plasmid containing the mouse HIF-1α IRES and coding region by *in vitro* transcription with T7 polymerase (Roche). Three times FLAG-EGFP or FLAG-DDX6 expressing HEK293 cells were harvested and lysed by lysis buffer. These proteins were immunoprecipitated by anti-FLAG agarose beads (Sigma). Immunoprecipitate-containing beads were mixed with 1 μl of *in vitro* transcripted RNA solution (0.4 μg/μl) at 4°C for 1 h. After washing the beads, RNA-bound proteins were eluted by 0.5 μg/μl FLAG peptide. Protein concentration was determined by the Bio-Rad protein assay reagent. Protein (1.4 μg) was subjected to SDS–polyacrylamide gel electrophoresis, and 3× FLAG-EGFP or FLAG-DDX6 expression was determined by western blots using anti-FLAG antibody. For RT–PCR analysis, 1.4 μg of protein containing RNA was incubated at 65°C for 10 min, 30°C for 5 min and then the RT enzyme was added and incubated at 42°C for 20 min, 95°C for 2 min and 4°C using the ExScript RT reagent kit (Takara). PCR was performed as follows: pre-denaturation at 94°C for 2 min, 30 cycles of denaturation at 94°C for 30 s and

annealing and extension at 68°C for 20 s. Primers are shown in Supplementary Table S3.

Immunocytochemistry

Cells were placed in hypoxic conditions for 48 h. Cells were fixed in 4% paraformaldehyde for 30 min and permeabilized with 0.1% Triton-PBS for 3 min at room temperature. After washing three times with 3% (weight/volume) BSA/PBST, cells were incubated with primary antibodies overnight at 4°C. Cells were washed three times with PBST and incubated for 1 h with secondary antibodies in 3% BSA/PBST, and then washed three times with PBST. The nuclei of cells were counterstained with DAPI dissolved in PBS. Finally, cells were filled with PBST. Microscopy analyses were performed with a Fluoview FV1000 confocal laser scanning microscope (OLYMPUS). DDX6 was visualized with Alexa-546 conjugated goat anti-rabbit secondary antibody. MAP2 was visualized with Cy-2 conjugated anti-mouse secondary antibody.

In situ hybridization

Anti-sense and sense probes of pri-miR-130a (522 nt) were prepared as DIG-labeled nucleic acids. Probes of mature miR-130a (22 nt) and two mismatch mature miR-130a were prepared as DIG-labeled locked nucleic acids (Thermo). Paraffin-embedded blocks and sections of mouse embryos (E18.5) for *in situ* hybridization were obtained from Genostaff, Inc. (Japan). Hybridization was performed with DIG-labeled miR-130a probes at concentrations of 100 ng/ml in Probe Diluent (Genostaff) at 25°C for 24 h. The sections were incubated with an anti-DIG AP conjugate (Roche) for 2 h. Coloring reactions were performed overnight with NBT/BCIP (Roche). The sections were counterstained with Kernechtrot (Mutoh), dehydrated, and then mounted with Malinol (Mutoh). Pri-miR-130a probes and mature miR-130a locked nucleic acids probes are shown in Supplementary Table S4.

For HIF-1α mRNA expression in neuronal cells, Digoxigenin-labeled anti-sense and sense (control) probes (Supplementary Table S4) were obtained from Genostaff, Inc. Normoxia and hypoxia treated cells were fixed with 4% paraformaldehyde and permeabilized with 0.1% Triton-PBS for 2 min at room temperature. After washing three times with PBST, HIF-1α mRNA was hybridized with the probe (1 ng/ml) at 25°C overnight. After washing five times with pre-warmed PBST (at 37°C), cells were incubated with anti-digoxigenin antibody (Roche) at 25°C for 6 h. Cells were washed three times with PBST and incubated for 1 h with secondary antibodies, and then washed three times with PBST. The nuclei of cells were counterstained with DAPI dissolved in PBS. Finally, cells were filled with PBST. Microscopy analyses were performed with a Fluoview FV1000 confocal laser scanning microscope (OLYMPUS). DDX6 was visualized with Alexa-546 conjugated goat anti-rabbit secondary antibody. HIF-1α mRNA was visualized with Cy-2 conjugated anti-mouse secondary antibody.

Antibody, miRNA and siRNA

Antibodies recognizing HIF-1α (R&D systems), HIF-1β/ARNT1 (BD Biosciences), DDX6 (BETHYL), actin (CHEMICON), MAP2 and FLAG (Sigma) were used. For secondary antibodies, HRP-conjugated anti-mouse IgG (CHEMICON), peroxidase-conjugated anti-rabbit IgG (Sigma), Alexa-546-conjugated anti-rabbit IgG (Invitrogen) and Cy-2-conjugated anti-mouse IgG (Jackson ImmunoResearch) were used.

miRNA precursors (pre-miR-130a, pre-miR-130b and pre-miR negative control) were purchased from Ambion. miRIDIAN hairpin inhibitors (miR-130a inhibitor, miR-130b inhibitor and control) and FBXL11 siRNA were purchased from Dharmacon. Other siRNAs were purchased from QIAGEN. Target sequences for siRNAs are indicated in Supplementary Table S2. Transfection of these pre-miRNAs, miRIDIAN hairpin inhibitors and siRNAs were performed using DharmaFECT 1 transfection reagent (Dharmacon) according to the manufacturer's protocol.

RESULTS

miR-130a and -130b regulate HIF-1α signaling

To investigate HIF-1α translational regulation by miRNAs during hypoxia, we first searched the HIF-1α 3′UTR according to the miRbase database and found that 19 potential miRNAs were predicted (Supplementary Figure S1). Among these miRNAs, we selected and focused on the miR-130 family, which was recently reported to regulate angiogenesis through VEGF expression (25). Therefore, we examined whether the miR-130 family is involved in the HIF-1α pathway, including VEGF regulation. We found that HEK293 cells transfected with pre-miR-130a and -130b increased HIF-1α expression in a dose-dependent manner under hypoxia (Figure 1A and B). However, we could not detect HIF-1α expression in cells with pre-miR-130a and -130b under normoxia (Figure 1A). It remains possible that HIF-1α protein is degradated despite the presence of the miR-130 family, since it has been reported that HIF-1α is rapidly ubiquitinated in normoxia (4). Furthermore, it is known that HIF-1α interacts with HIF-1β as a heterodimeric transcription factor (26). We found that the miR-130 family did not affect HIF-1β expression under both conditions (Supplementary Figure S3A). In fact, HIF-1β 3′UTR does not contain the miR-130 family binding site (Supplementary Figure S2), and HIF-1β has nucleotide sequence identities of only 23% with HIF-1α. We also observed that the endogenous mature forms of miR-130a and -130b increased under hypoxia in HEK293 cells (Figure 1C), and that HIF-1α expression during hypoxia was decreased with the addition of 200 nM of miR-130a and -130b inhibitors (Figure 1D).

Next, we examined HIF-1α activity in the presence of pre-miR-130a and -130b. We used an HRE-luciferase reporter gene (pHRE-Luc) which has six tandem repeats of the HIF-1α-binding sequence from the transferrin

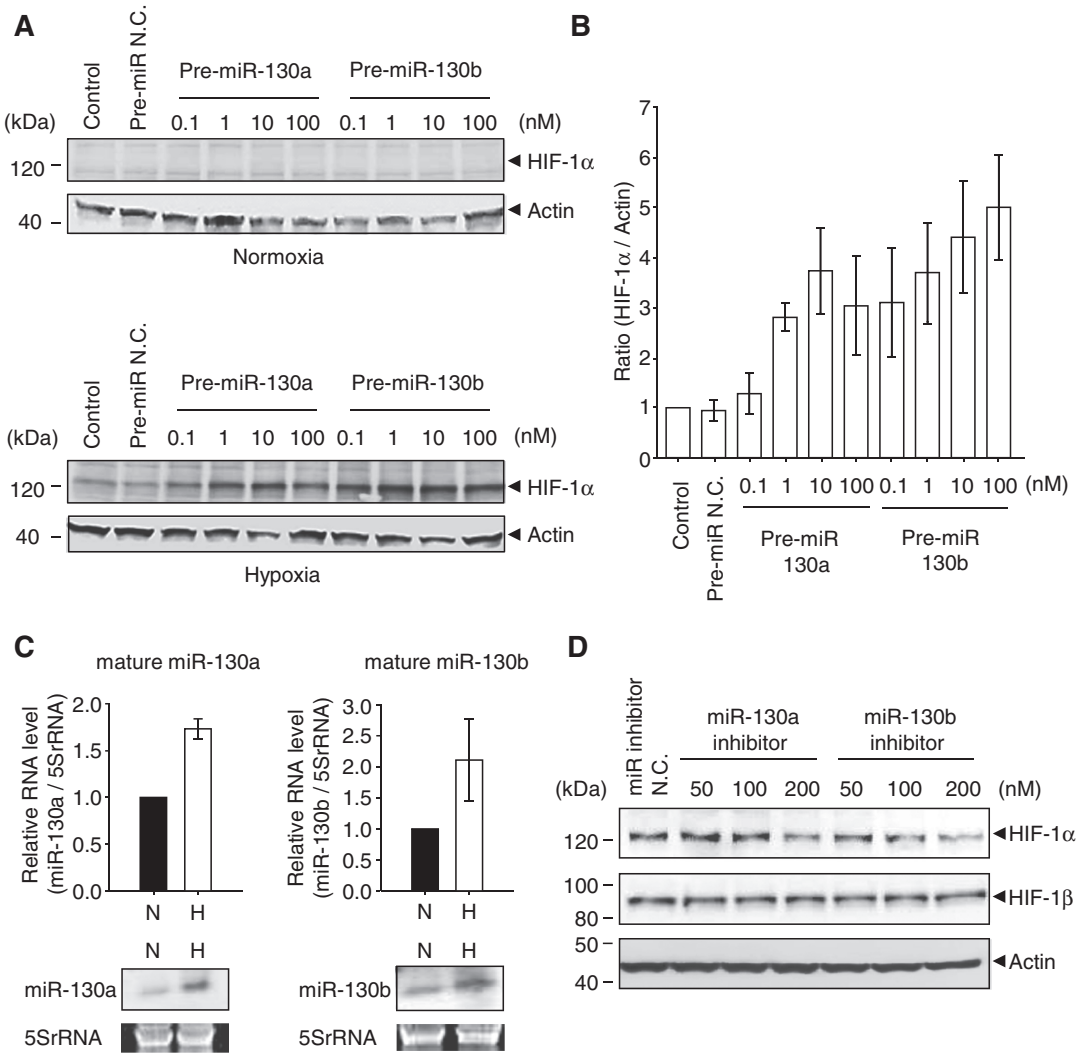

Figure 1. Effects of the miR-130 family on HIF-1α expression. (**A**) HEK 293 cells were transfected with 0.1–100 nM of pre-miR-130a and -130b for 48 h, and then cells were exposed to hypoxia for 8 h. Expression levels of HIF-1α and actin were detected by western blot. Pre-miR negative control (pre-miR N.C.) was 100 nM. Left lane (control) shows untransfected cells. (**B**) HIF-1α expression levels under hypoxia shown in (A) were calculated by the relative expression to actin. The ratio to the control is the mean of four independent experiments ± SD. (**C**) Endogenous mature miR-130a (top panel, left) and -130b (top panel, right) levels were detected by qRT–PCR. RNA levels for miR-130a and -130b were normalized by 5S rRNA. Solid bars and open bars show normoxia (N) and hypoxia (H), respectively. The ratio to normoxia is the mean of three independent experiments ± SD. Northern blot analyses of mature miR-130a and -130b are shown in the bottom panels. (**D**) HEK 293 cells were transfected with 50, 100 and 200 nM of miRIDIAN miR-130a and -130b inhibitors for 6 h, and then cells were exposed to hypoxia for 48 h. HIF-1α and HIF-1β expression levels were detected by western blot. A miRIDIAN miR inhibitor N.C.(200 nM) was used as a control.

receptor promoter. HRE-mediated luciferase activity was significantly enhanced by miR-130a and -130b during hypoxia, while a slightly increased level of luciferase was observed in normoxia (Figure 2A). Since the luciferase assay is more sensitive than the western blot, it may enable the detection of some HIF-1α activity in the absence of detectable HIF-1α protein under normoxia. Further, we examined NFκ-B signaling, since NFκ-B is the key component of VEGF-induced angiogenesis in many tumors (27). However, pre-miR-130a and -130b did not influence the NFκ-B reporter gene (Figure 2B). We also confirmed that the levels of endogenous VEGF mRNA in the presence of pre-miR-130a and -130b were two times higher than that of the control under hypoxia (Figure 2C). These results indicate that elevation of miR-130a and -130b is involved in the regulation of HIF-1α-induced transactivation of target genes under hypoxia.

The miR-130 family targets DDX6

To determine whether miR-130a and -130b induce HIF-1α expression through interactions with the HIF-1α 3′UTR, we examined luciferase expression using a Luc-HIF-1α 3′UTR reporter gene. The results of the reporter assay indicated that pre-miR-130a and -130b had slightly increased luciferase expression (Supplementary Figure S3B). These results suggested that miR-130b had some

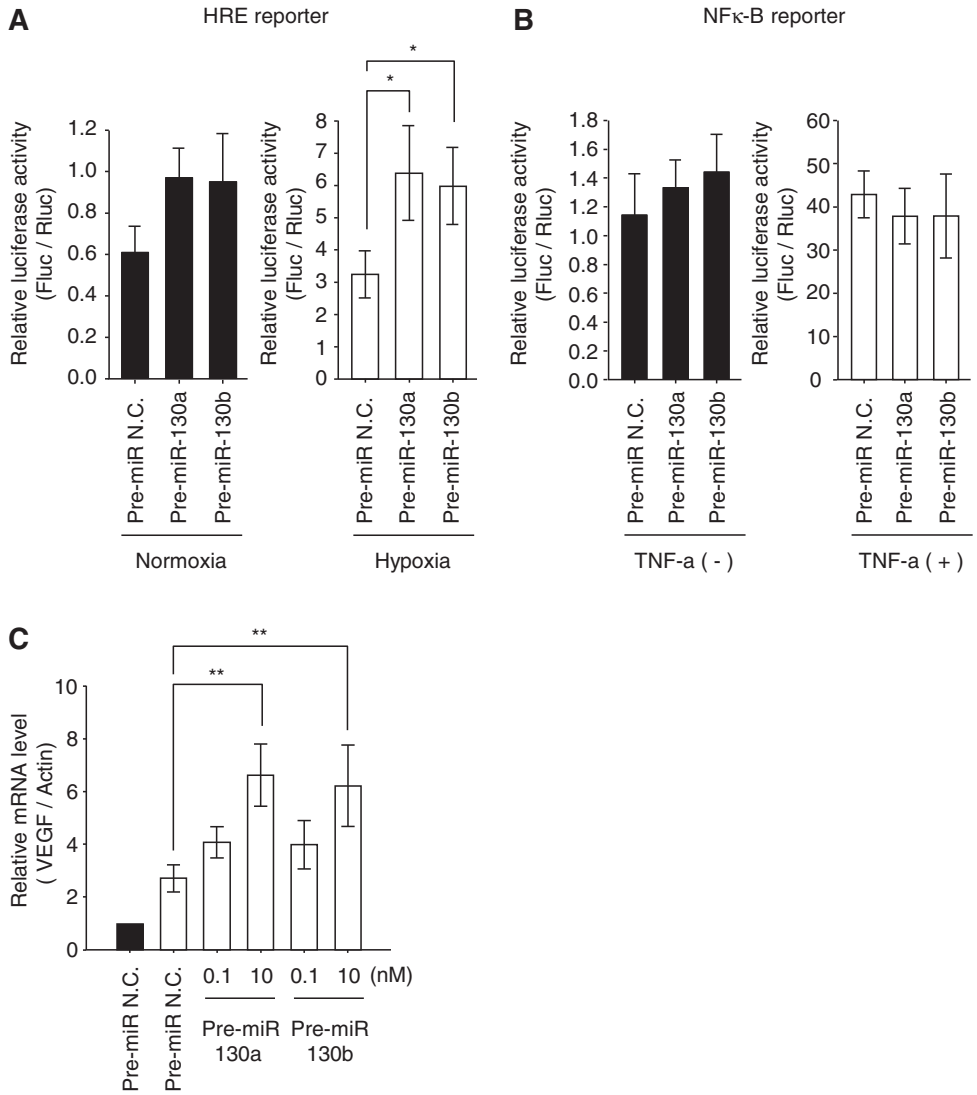

Figure 2. Hypoxia signaling in the miR-130 family. (**A** and **B**) Reporter assays with HRE reporter plasmid or NF-κB reporter plasmid are shown. HEK293 cells were transfected with reporter plasmid and pre-miR-130 family members (10 nM). After 48 h transfection Cells were exposed to hypoxia (A, open bars) or 20 ng/ml TNF-α for 12 h (B, open bars). Data are presented as means ± SD ($n = 5$, $*P < 0.01$). Solid bars show the luciferase activity without treatment in the pre-miR N.C. and pre-miR-130a family members (solid bars). The *P*-values in the left of (A) are as follows: Control versus 130a: $P = 0.04$; control versus 130b: $P = 0.02$. Firefly luciferase activities were analyzed and corrected for transfection efficiency by the Renilla luciferase activity. (**C**) In the transient transfection of pre-miRNAs (0.1 and 10 nM), after 48 h cells were exposed to hypoxia, and VEGF mRNA levels were analyzed by qRT–PCR. The mRNA levels were corrected for differences in β-actin mRNA. The values during hypoxia (open bars) are represented as the ratio of control in normoxia (solid bars). Results are presented as means ± SD ($n = 6$, $**P < 0.001$). Pre-miR N.C. (10 nM) was used as a control.

effect on HIF-1α induction through interactions with the HIF-1α 3′UTR. To identify the target genes of miR-130a and -130b that strongly influence HIF-1α expression, we focused on commonly observed genes and highly ranked genes in four databases (Target Scan, Pictar, miRanda and miRbase). We investigated nine genes, excepting the MEOX2/GAX gene that has already been reported as an miR-130a target (19) (Supplementary Table S1). As five of nine genes resulted in inefficient knock-down, we found that among the four candidate genes (PHF, TNRC6A, DDX6 and RSN), knock-down of the DDX6 gene strongly enhanced HIF-1α (Supplementary Figure S4). In fact, the expression of a luciferase reporter gene containing the DDX6 3′UTR was decreased by miR-130a and -130b (Figure 3B, left), but a DDX6 3′UTR mutant at the miR-130a- and -130b-binding site (Figure 3A) showed no change in luciferase activity (Figure 3B, right). Furthermore, endogenous DDX6 protein levels were down-regulated by pre-miR-130a and -130b (Figure 3C). In contrast, overexpression of DDX6, but not knock-down of DDX6, decreased HIF-1α expression (Figure 3D). These results suggested that HIF-1α expression was regulated by the miR-130 family through DDX6.

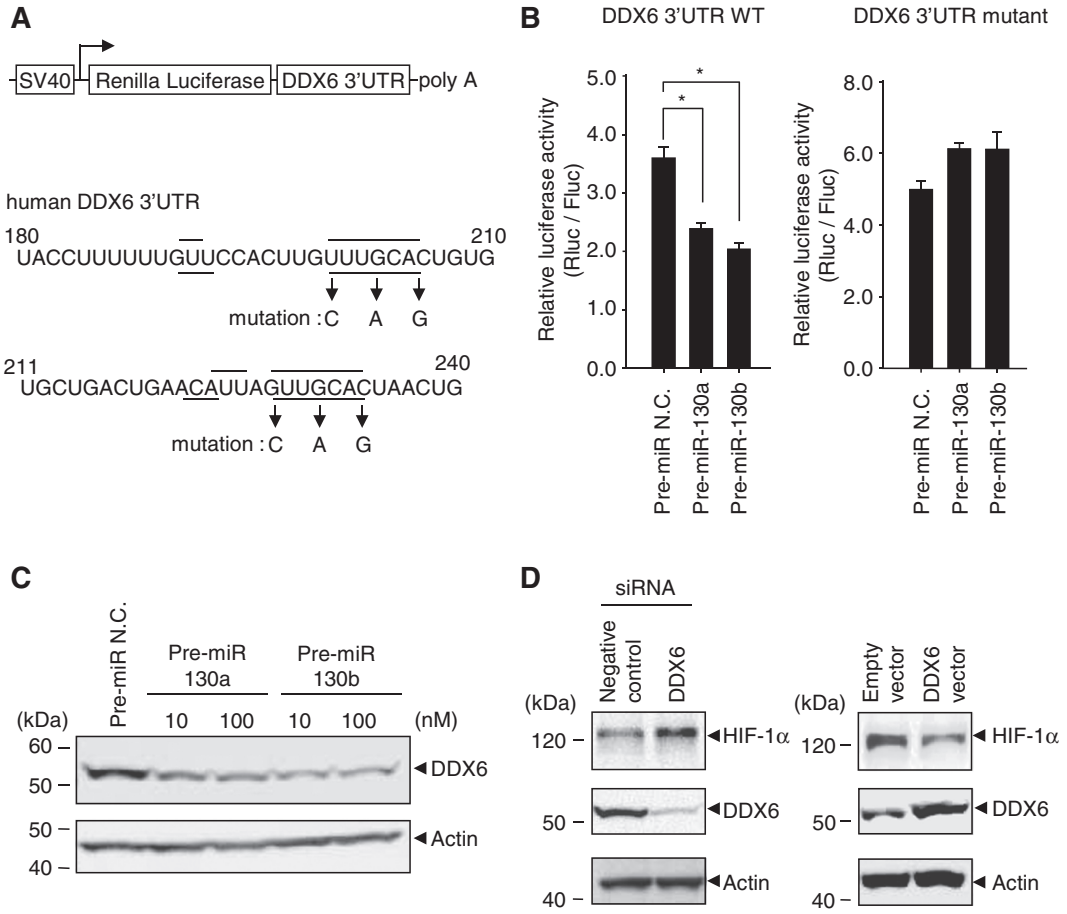

Figure 3. Regulation of HIF-1α translation by DDX6. (**A**) The DDX6 mRNA 3′UTR sites targeted by miR-130a (line) and -130b (dotted line) are shown. Mutagenesis of the DDX6 mRNA 3′UTR is indicated by arrows. (**B**) HEK293 cells were transfected with pre-miRNAs (25 nM) and either DDX6 3′UTR wild-type (left) or mutant (right) reporter genes, and then cells were cultured under normoxia. After 48 h, luciferase activities were analyzed and Renilla luciferase expression was normalized to firefly luciferase. Results represent means ± SD ($n = 6$, $^*P < 0.0001$). (**C**) Endogenous DDX6 expression levels in the transfection of pre-miR-130a and -130b under normoxia were detected by western blots. Pre-miR N.C. was 100 nM. (**D**) Negative control and DDX6 siRNAs (50 nM) were transfected into HEK293 cells. After 8 h of hypoxia, HIF-1α expression levels were detected by western blots (left panel). The right panel shows HIF-1α expression in overexpression of DDX6.

DDX6 effect on the HIF-1α IRES element

Since it has been reported that DDX6 (also known as rck/p54), an RNA helicase, functions as an IRES translational repressor (28), we examined whether HIF-1α IRES activity was induced by decreasing DDX6 through miR-130a and -130b. We used a Renilla-HIF-1α IRES-FireFly (pRhifF) luciferase reporter gene (Figure 4A), which has an HIF-1α IRES sequence inserted into the dicistronic vector pRF containing the Renilla and FireFly luciferase genes (8). We found that transfection of pre-miR-130a and -130b had little effect on the pRF reporter gene (Figure 4B, left), while pre-miR-130a and -130b significantly increased the reporter activity in the presence of HIF-1α IRES (Figure 4B, right). The same results were found in DDX6 knock-down experiments (Figure 4C). Furthermore, our results indicated that immunoprecipitation of endogenous DDX6 included endogenous HIF-1α mRNAs (Figure 4D). In the binding assay of *in vitro* transcribed RNA and FLAG-DDX6, we found that DDX6 specifically bound to the HIF-1α IRES element (259 nt) in the 5′UTR (Figure 4E, left), but not to the HIF-1α coding region (Figure 4E, right). From these results, we conclude that the increase of HIF-1α expression is attributable to the interaction between DDX6 and the HIF-1α IRES element.

Hypoxic stress suppresses DDX6 in neuronal cells

It has been shown that miR-130a expression is predominant in old mouse cerebellums, although miR-130a has little expression in the cortex (29). We investigated the tissue distribution of pri-miR-130a and mature miR-130a. *In situ* hybridization revealed that pri-miR-130a was expressed in the cortex, cerebellum and kidneys in E18.5 mice (Supplementary Figure S6). Mature miR-130a had the same pattern as pri-miR-130a, which was expressed in the granule cells of the cortex, cerebellum and the renal tubes of the kidneys (Figure 5A and B). The mature form of miR-130a in neuronal cells was increased under hypoxia; however,

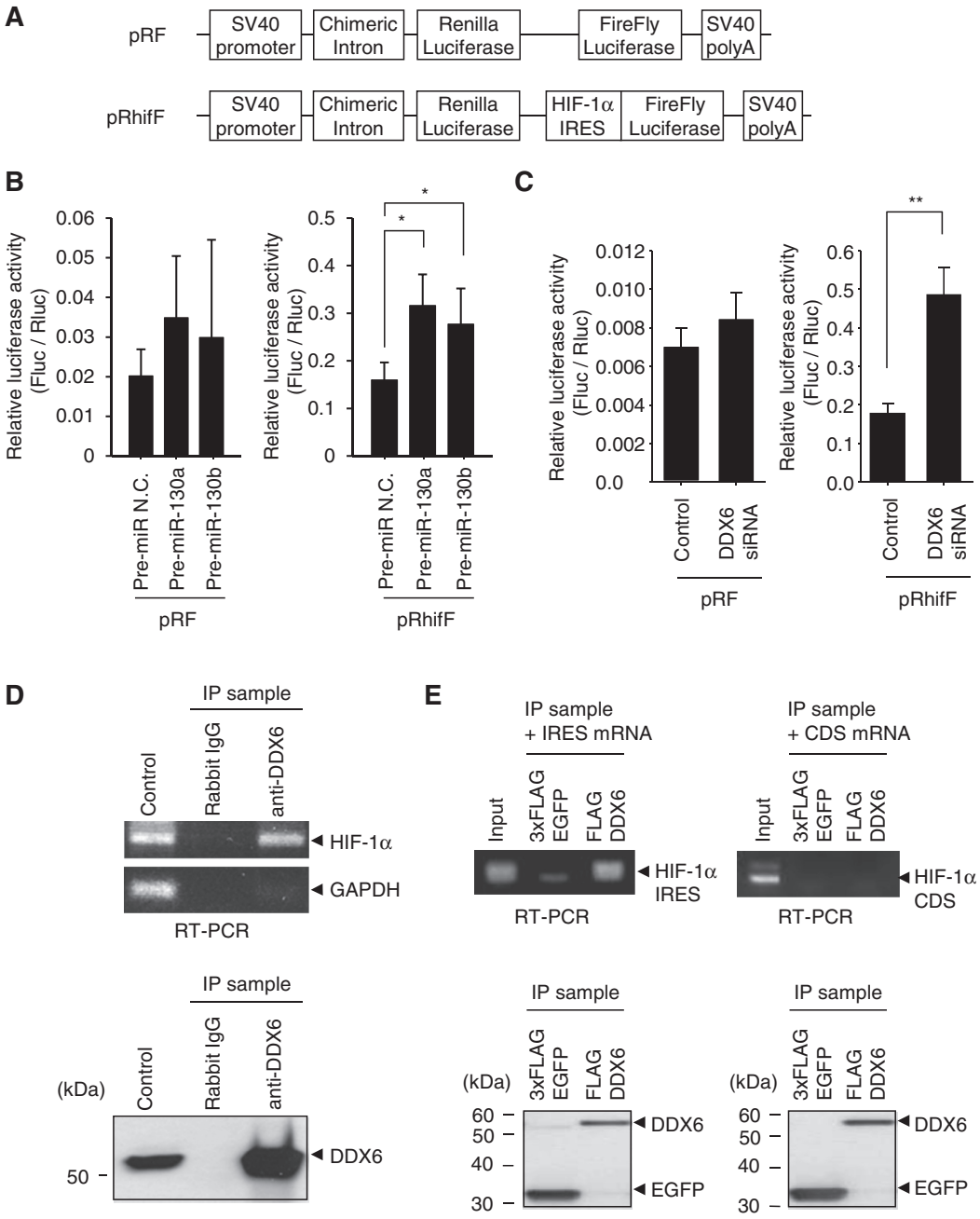

Figure 4. Binding of DDX6 to HIF-1α IRES. (**A**) Schematic representation of the dicistronic pRF and pRhifF vector. pRhifF has an HIF-1α IRES between the Renilla and firefly luciferase genes. (**B** and **C**) HEK293 cells were treated with pre-miRNAs (50 nM) or DDX6 siRNA (50 nM) and then transfected with either pRF or pRhifF reporter plasmids. Cells were cultured under normoxia and luciferase activities were analyzed. Reporter activity is represented as the ratio of firefly to Renilla luciferase. Results represent means ± SD ($n = 6$, $*P < 0.01$, $**P < 0.001$). The left of (**B**) does not meet the significance level ($n = 6$; Control versus 130a: $P = 0.1$, control versus 130b: $P = 0.4$). (**D**) Endogenous DDX6 was immunoprecipitated by anti-DDX6 antibodies or normal rabbit IgG (top panel). HIF-1α or GAPDH mRNA associated with endogenous DDX6 was analyzed by RT–PCR of immunoprecipitates (IP sample). RT–PCR was also performed for 1 μg of total RNA (control). The bottom panel shows immunoprecipitates (IP sample) by western blots using anti-DDX6 antibody. Left lane (control) shows DDX6 expression in whole cell lysates (20 μg of protein). (**E**) *In vitro* binding assay of the synthetic mRNA and DDX6. Anti-FLAG agarose binding 3×FLAG-EGFP or FLAG-DDX6 were mixed with the *in vitro* transcribed HIF-1α IRES mRNA (259 nt) and a portion of the HIF-1α-coding region mRNA (CDS, 437 nt). These eluates with FLAG peptides were detected by RT–PCR. RNA input amounts were used as the binding assay. The bottom panel shows immunoprecipitates (IP sample) by western blots using anti-FLAG antibody.

the levels of the pri and pre forms were no different between normoxia and hypoxia (Figure 5C). Several studies have reported that miR-130a is insensitive to hypoxia in HUVEC, colon cancer and breast cancer cell lines (30,31), whereas miR-130a expression is upregulated by mitogens and proangiogenesis factors in HUVEC (25). We found that HeLa and NIH-3T3 cell lines also showed no increase in the mature forms of miR-130a and -130b

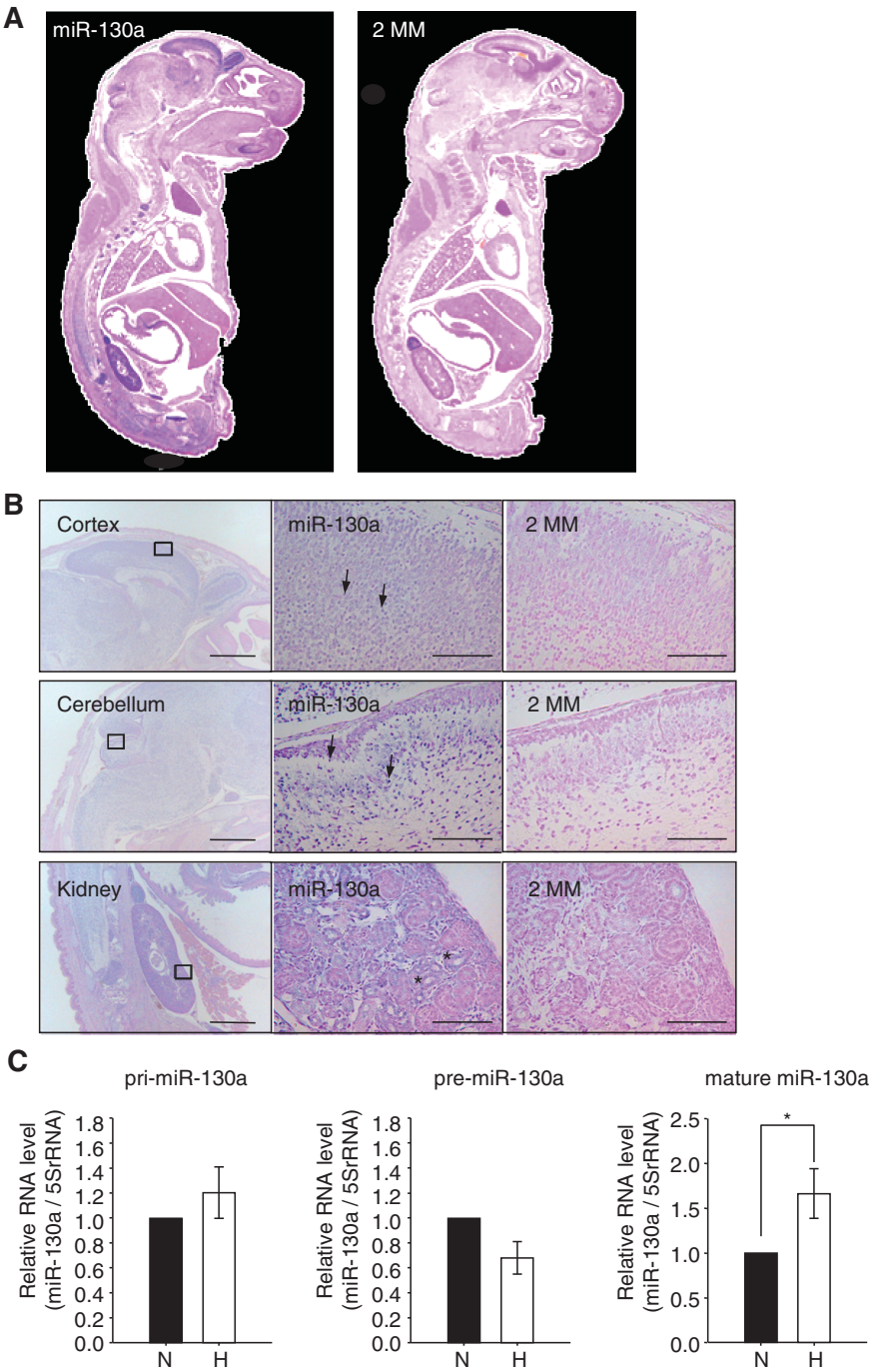

Figure 5. Tissue distribution of mature miR-130a. (**A**) *In situ* hybridization experiment on cryosections of E18.5 mouse embryos. Expression of mature miR-130a was investigated by LNA-modified anti-sense probes that recognize mature miR-130a (left). Right panel shows hybridization using LNA-modified anti-sense probes with 2 nt of the mature miR-130a substituted (2MM). (**B**) Mature miR-130a was expressed in the cortex (top panel, left), cerebellum (middle panel, left) and kidneys (bottom panel, left). Scale bar = 1 mm. Squares represent areas shown at higher magnifications. Granule cells in the cortex and cerebellum are indicated by arrowheads. Renal tubes in kidney are indicated by asterisks. Scale bar = 100 µm. (**C**) Hippocampus neuronal cells were cultured under normoxia (solid bars) or hypoxia (open bars) for 72 h. Levels of endogenous pri, pre and mature forms of miR-130a were detected by qRT–PCR. RNA levels were normalized by 5S rRNA. The ratio to normoxia is the mean of five independent experiments ± SD (*$P < 0.01$).

under hypoxia (Supplementary Figure S7). Thus, miR-130a response and processing occur in a cell type-specific manner under hypoxic conditions.

Moreover, DDX6 was detected in discrete cytoplasmic foci, referred to as P-bodies in neuronal cells (Figure 6A), since DDX6 was co-localized with Dcp1a which is a P-bodies marker (Supplementary Figure S8A). Under hypoxia for 48 h, DDX6 was reduced and the focus number was significantly decreased in primary cultured neurons (Figure 6A and B). These observations were

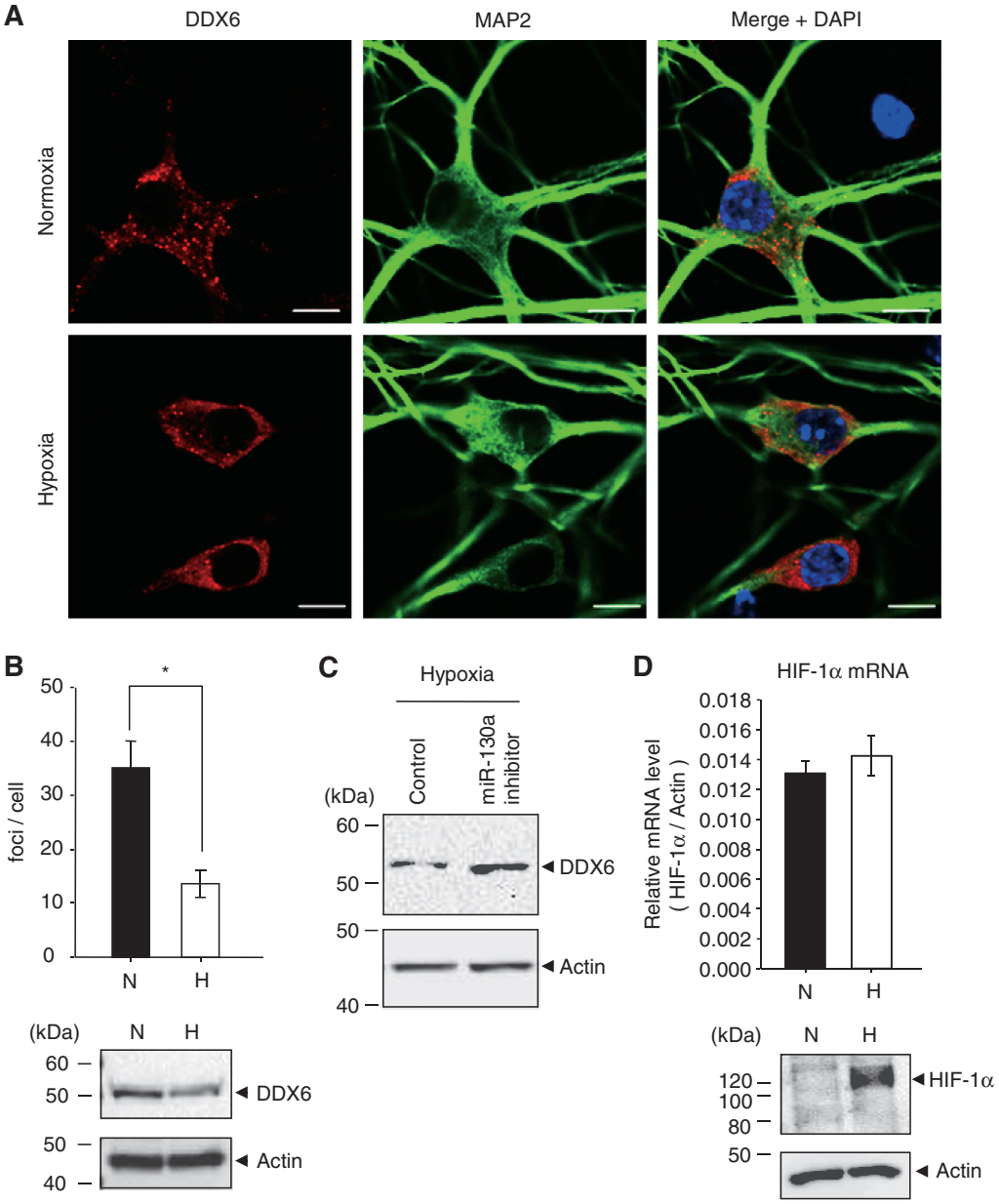

Figure 6. P-body formation in neurons under hypoxia. (**A**) After exposure to normoxia (top panel) and hypoxia (bottom panel) for 48 h, cells were stained with DDX6 antibody or MAP2 antibody as a neuronal marker. Nuclei were stained with DAPI. Scale bar = 10 μm. (**B**) The mean number of P-bodies per cell under normoxia (solid bars) and hypoxia (open bars) are shown. Results represent means ± SE ($n = 10$, $^*P < 0.0001$). The bottom panel shows endogenous DDX6 expression levels in hippocampus neuronal cells under normoxia (N) and hypoxia (H) for 48 h. (**C**) Hippocampus neuronal cells were transfected with 50 nM of miRIDIAN miR-130a inhibitor for 48 h, and then cells were exposed to hypoxia for 72 h. DDX6 expression levels were detected by western blotting. Similar results were obtained in two independent experiments. (**D**) After exposure to normoxia (N, solid bar) and hypoxia (H, open bar) for 48 h, HIF-1α mRNA levels were measured by qRT–PCR. The values were corrected by β-actin mRNA. Results are presented as means ± SD ($n = 3$). The bottom panel shows endogenous HIF-1α expression levels in hippocampus neuronal cells under normoxia (N) and hypoxia (H) for 48 h.

also made in HEK293 cells (Supplementary Figure S5). We also found that DDX6 mRNA was at the same level under normoxia and hypoxia (Supplementary Figure S8B), and that 50 nM of miR-130a inhibitor suppressed the down-regulation of DDX6 under hypoxia in neurons (Figure 6C). These results suggested that DDX6 is down-regulated by miR-130a at the post-transcriptional level under hypoxia. In these hypoxic conditions, HIF-1α protein accumulated in neuronal cells, and HIF-1α mRNA levels were not significantly different between normoxia and hypoxia (Figure 6D).

Thus, to determine whether HIF-1α expression was modulated by the interaction with DDX6 in neuronal cells, we examined the co-localization of endogenous HIF-1α mRNA and DDX6 by fluorescence *in situ* hybridization (Figure 7A). HIF-1α mRNA was observed in cell

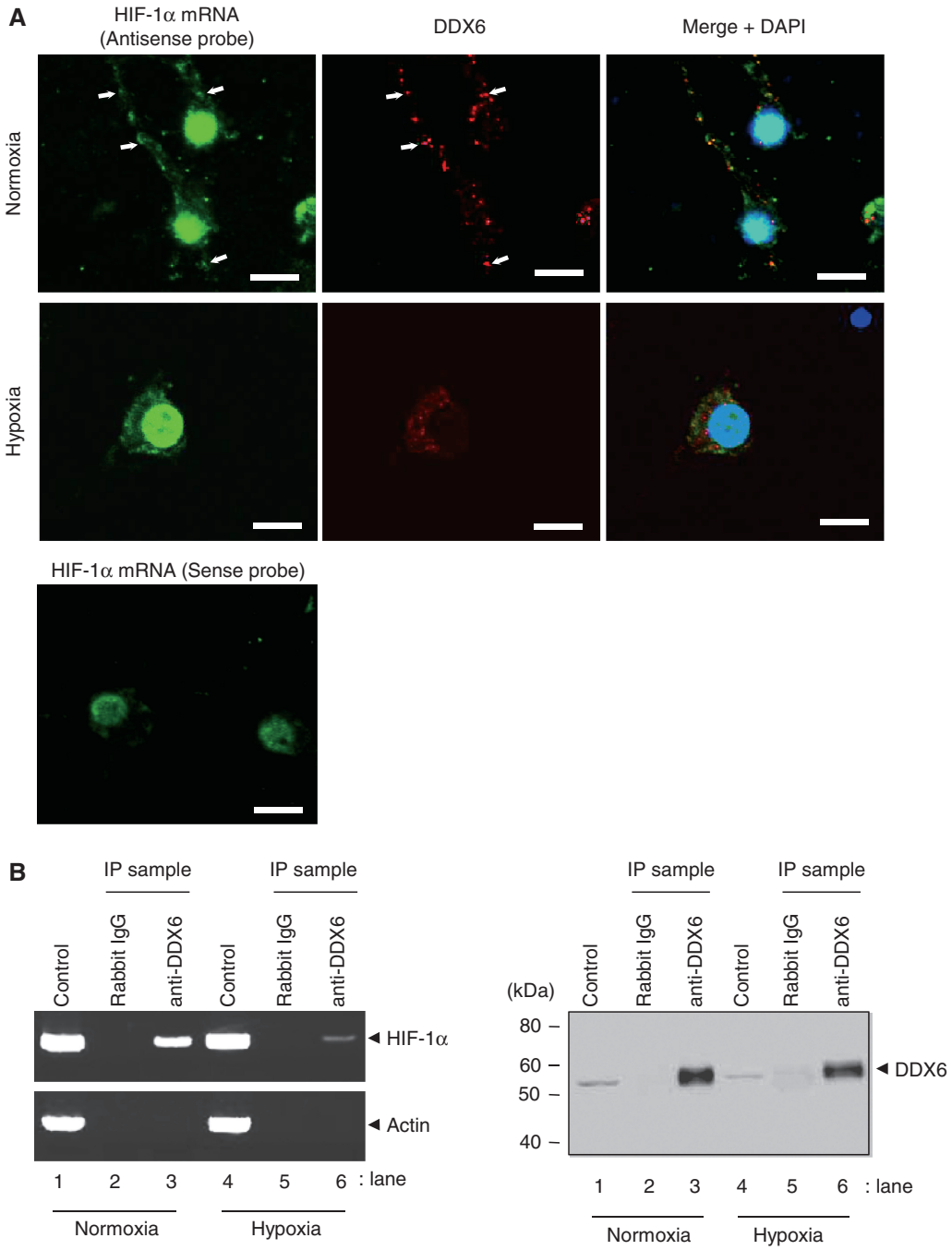

Figure 7. HIF-1α mRNA localization in neuronal cells. (**A**) After exposure to normoxia (top panel) and hypoxia (middle panel) for 48 h, HIF-1α mRNA expression was examined by fluorescence *in situ* hybridization in neuronal cells, and then cells were stained with DDX6 antibody and nuclei marker DAPI. The co-localization of both HIF-1α mRNA and DDX6 foci are indicated by arrowheads. The bottom panel shows non-specific staining by HIF-1α RNA sense probe. Scale bar = 10 μm. (**B**) After neuronal cells were exposed to normoxia (lanes 1, 2 and 3) and hypoxia (lanes 4, 5 and 6) for 48 h, endogenous DDX6 was immunoprecipitated by anti-DDX6 antibodies or normal rabbit IgG (left panel). HIF-1α or actin mRNA associated with endogenous DDX6 was analyzed by RT–PCR of immunoprecipitates (IP sample). RT–PCR was also performed for 1 μg of total RNA (control). The right panel shows immunoprecipitates (IP sample) by western blotting using anti-DDX6 antibody. Lanes 1 and 4 (control) show DDX6 expression in whole-cell lysates (20 μg of protein).

bodies, dendrites and nuclei, although the nuclei included non-specific binding in a reaction with the HIF-1α mRNA sense probe. We found that HIF-1α mRNA foci were co-localized with DDX6 foci under normoxia (Figure 7A, top). However, there were very few HIF-1α mRNA foci in dendrites under hypoxia, and HIF-1α mRNA was abundant in the cell bodies. DDX6 foci were also decreased and the co-localization of HIF-1α mRNA and DDX6 was decreased under hypoxia (Figure 7A, middle). Furthermore, we examined whether HIF-1α mRNA that immunoprecipitated with endogenous DDX6 was decreased under hypoxia. As shown in

Figure 7B, HIF-1α mRNA under hypoxia was decreased in the immunoprecipitates of DDX6 compared to those under normoxia (Figure 7B, left, lanes 3 and 6). These results suggest that HIF-1α mRNA does not assemble with P-bodies under hypoxia due to a decrease of DDX6 by miR-130a.

DISCUSSION

In this study, we first described the regulation of HIF-1α translation during prolonged hypoxia by the miR-130 family and DDX6. As recent studies have reported that miRNAs function both as inducers and suppressors of translation (18), we hypothesized that HIF-1α expression under hypoxia was enhanced by the miR-130a family and the Ago complex thorough stimulation of the HIF-1α 3′UTR. However, contrary to our hypothesis, miR-130a and -130b regulated DDX6 to affect HIF-1α expression rather than directly influencing HIF-1α translation under hypoxia. It has been reported that DDX6 (rck/p54) negatively regulates c-myc expression and leads to a reduction of c-myc IRES-dependent translation (28). The IRES of the c-myc P2 5′UTR is unwound by DDX6. In addition, recent work has shown that DDX6 broadly regulates mRNA translation as a general translational repressor (32). Although it is unclear whether DDX6 preferentially interacts with the IRES element rather than general mRNA, our studies indicated that DDX6 binds to HIF-1α IRES elements, and a reduction of DDX6 results in an increase in HIF-1α expression. These results may suggest that the HIF-1α IRES structure is also unwound by DDX6, causing translational inhibition. However, the interaction site and binding structure of DDX6 in the c-myc IRES and the HIF-1α IRES are not yet fully understood. We also cannot rule out the possibility that the protein complex containing DDX6 affects IRES elements, since DDX6 interacts with translational initiation factor eIF4E, decapping enzyme Dcp1a and P-body components.

P-bodies have dynamic structures requiring not only mRNA decay, but also permitting the re-entry of stored mRNAs into the translation pathway (33). In addition, P-bodies can assemble and disassemble in response to stress, such as amino acid starvation, oxidative stress and endoplasmic reticulum stress (34). Knock-down of DDX6 decreases the number of GW/P-bodies (35). Therefore, our results suggest that when neuronal cells are exposed to hypoxia, the DDX6-HIF-1α mRNA complex disassembles for translational initiation of HIF-1α. We also found that P-bodies were formed in a reversible manner between normoxia and hypoxia because of the increase of P-bodies in reoxygenation (Supplementary Figure S8). Furthermore, it is known that DDX6 is also a component of stress granules (SG). Our results indicated that DDX6 was colocalized with the SG marker TIAR upon arsenite-induced oxidative stress (Supplementary Figure S9). However, TIAR foci in the cytoplasm were not observed under normoxia, hypoxia or reoxygenation in neuronal cells. Further investigation is needed to determine the molecular mechanism underlying HIF-1α translation and the induction of P-bodies, including the DDX6 component.

We also found that the mature form of miR-130a was increased under hypoxia. However, the levels of pri and pre forms were not significantly changed under normoxia and hypoxia. Ago2 has been reported to be constitutively expressed under hypoxia (36). Given reports showing that knock-downs of Drosha or Ago2 accumulate the pri or pre forms and diminish the mature forms (37,38), our data suggest that miR-130a processing occurs in neuronal cells under hypoxia. It is of interest whether Ago2 or other RNAase III members have enzyme activity under hypoxia.

In conclusion, our findings in this study support a translational mechanism of HIF-1α through miR-130 and DDX6. First, HIF-1α mRNA levels were not influenced by the miR-130 family under normoxic and hypoxic conditions (Supplementary Figure S3C). Second, the miR-130 family suppressed DDX6 expression (Figure 3). Third, the HIF-1α IRES element revealed an association with DDX6 (Figures 4 and 7B). Fourth, HIF-1α mRNA foci were co-localized with P-bodies including DDX6 under normoxia, whereas P-body and HIF-1α mRNA assembly was reduced under hypoxia (Figure 7). Given all the evidence, we propose a mechanism (Figure 8) whereby HIF-1α mRNA is tethered by P-bodies in normoxic conditions. Under hypoxia, HIF-1α mRNA is released from the P-bodies or does not enter into P-bodies through decreased DDX6, which is regulated by the miR-130 family. In this way, HIF-1α translation, which depends on IRES, is induced by preventing regulation from translational repressor DDX6 under hypoxia. It might also be that this mechanism facilitates HIF-1α translation by PTB, HuR, 4E-BP1 and eIF4G as translational inducers. Our results imply that miR-130a may be involved in the pathology of ischemic diseases such as stroke. Further study of the translational regulation

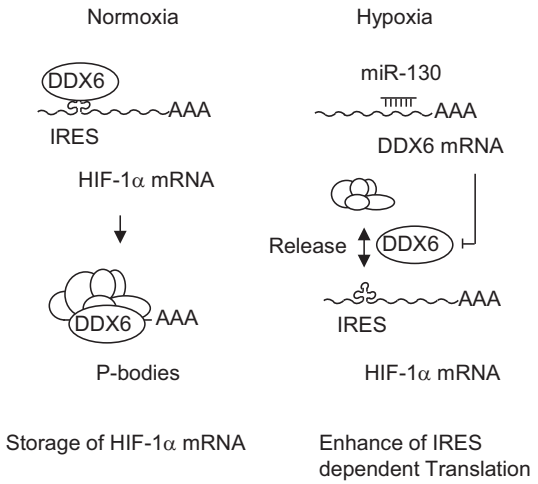

Figure 8. Illustration of DDX6 and HIF-1α regulation by miR-130. HIF-1α mRNA is accompanied by DDX6 to P-bodies which restrict translation with other P-body components under normoxia. Under hypoxia, DDX6 protein levels are decreased by the miR-130 family, and then HIF-1α is released from the P-bodies and facilitates IRES-dependent translation.

caused by DDX6 and the miR-130 family will lead to new insights into the physiology and pathogenesis of hypoxia.

SUPPLEMENTARY DATA

Supplementary Data are available at NAR Online.

ACKNOWLEDGEMENTS

We thank Dr G. J. Goodall (University of Adelaide, Australia) for providing the pRF and pRhifF reporter plasmids. We are grateful to Dr K. Nakamura, S. Kamijo and R. Tsuchiya (MITILS) for mouse support. We also thank Dr. T. Imai, Dr. H. Okano (Keio University) and the members of the Matsushita Lab for advice on experiments, technical assistance, and critical evaluation of this manuscript.

FUNDING

Ministry of Education, Culture, Sports, Science and Technology (MEXT) in Japan (to M.M.); Mitsubishi Kagaku Institute of Life Sciences (MITILS). Funding for open access charge: Grants-in-aid for scientific research from the Ministry of Education, Culture, Sports, Science and Technology (MEXT) in Japan.

Conflict of interest statement. None declared.

REFERENCES

1. Semenza,G.L. (1999) Perspectives on oxygen sensing. *Cell*, **98**, 281–284.
2. Semenza,G.L. (2001) Hypoxia-inducible factor 1: oxygen homeostasis and disease pathophysiology. *Trends Mol. Med.*, **7**, 345–350.
3. Spriggs,K.A., Bushell,M. and Willis,A.E. (2010) Translational regulation of gene expression during conditions of cell stress. *Mol. Cell*, **40**, 228–237.
4. Ivan,M., Kondo,K., Yang,H., Kim,W., Valiando,J., Ohh,M., Salic,A., Asara,J.M., Lane,W.S., Kaelin,W.G. Jr *et al*. (2001) HIFalpha targeted for VHL-mediated destruction by proline hydroxylation: implications for O2 sensing. *Science*, **292**, 464–468.
5. Lando,D., Peet,D.J., Whelan,D.A., Gorman,J.J. and Whitelaw,M.L. (2002) Asparagine hydroxylation of the HIF transactivation domain a hypoxic switch. *Science*, **295**, 858–861.
6. Jaakkola,P., Mole,D.R., Tian,Y.M., Wilson,M.I., Gielbert,J., Gaskell,S.J., Kriegsheim,A.v., Hebestreit,H.F., Mukherji,M., Schofield,C.J. *et al*. (2001) Targeting of HIF-alpha to the von Hippel-Lindau ubiquitylation complex by O2-regulated prolyl hydroxylation. *Science*, **292**, 468–472.
7. Laughner,E., Taghavi,P., Chiles,K., Mahon,P.C. and Semenza,G.L. (2001) HER2 (neu) signaling increases the rate of hypoxia-inducible factor 1alpha (HIF-1alpha) synthesis: novel mechanism for HIF-1-mediated vascular endothelial growth factor expression. *Mol. Cell. Biol.*, **21**, 3995–4004.
8. Lang,K.J., Kappel,A. and Goodall,G.J. (2002) Hypoxia-inducible factor-1alpha mRNA contains an internal ribosome entry site that allows efficient translation during normoxia and hypoxia. *Mol. Biol. Cell*, **13**, 1792–1801.
9. Galban,S., Kuwano,Y., Pullmann,R. Jr, Martindale,J.L., Kim,H.H., Lal,A., Abdelmohsen,K., Yang,X., Dang,Y., Liu,J.O. *et al*. (2008) RNA-binding proteins HuR and PTB promote the translation of hypoxia-inducible factor 1alpha. *Mol. Cell. Biol.*, **28**, 93–107.
10. Schepens,B., Tinton,S.A., Bruynooghe,Y., Beyaert,R. and Cornelis,S. (2005) The polypyrimidine tract-binding protein stimulates HIF-1alpha IRES-mediated translation during hypoxia. *Nucleic Acids Res.*, **33**, 6884–6894.
11. Braunstein,S., Karpisheva,K., Pola,C., Goldberg,J., Hochman,T., Yee,H., Cangiarella,J., Arju,R., Formenti,S.C. and Schneider,R.J. (2007) A hypoxia-controlled cap-dependent to cap-independent translation switch in breast cancer. *Mol. Cell*, **28**, 501–512.
12. Ambros,V. (2004) The functions of animal microRNAs. *Nature*, **431**, 350–355.
13. Brodersen,P. and Voinnet,O. (2009) Revisiting the principles of microRNA target recognition and mode of action. *Nat. Rev. Mol. Cell Biol.*, **10**, 141–148.
14. Palatnik,J.F., Wollmann,H., Schommer,C., Schwab,R., Boisbouvier,J., Rodriguez,R., Warthmann,N., Allen,E., Dezulian,T., Huson,D. *et al*. (2007) Sequence and expression differences underline functional specialization of Arabidopsis microRNAs miR159 and miR319. *Dev. Cell*, **13**, 115–125.
15. Eulalio,A., Huntzinger,E. and Izaurralde,E. (2008) Getting to the root of miRNA-mediated gene silencing. *Cell*, **132**, 9–14.
16. Liu,J., Valencia-Sanchez,M.A., Hannon,G.J. and Parker,R. (2005) MicroRNA-dependent localization of targeted mRNAs to mammalian P-bodies. *Nat. Cell Biol.*, **7**, 719–723.
17. Llave,C., Xie,Z., Kasschau,K.D. and Carrington,J.C. (2002) Cleavage of Scarecrow-like mRNA targets directed by a class of Arabidopsis miRNA. *Science*, **297**, 2053–2056.
18. Vasudevan,S., Tong,Y. and Steitz,J.A. (2007) Switching from repression to activation: microRNAs can up-regulate translation. *Science*, **318**, 1931–1934.
19. Jopling,C.L., Schutz,S. and Sarnow,P. (2008) Position-dependent function for a tandem microRNA miR-122-binding site located in the hepatitis C virus RNA genome. *Cell Host Microb.*, **4**, 77–85.
20. Jopling,C.L., Yi,M., Lancaster,A.M., Lemon,S.M. and Sarnow,P. (2005) Modulation of hepatitis C virus RNA abundance by a liver-specific MicroRNA. *Science*, **309**, 1577–1581.
21. Bhattacharyya,S.N., Habermacher,R., Martine,U., Closs,E.I. and Filipowicz,W. (2006) Relief of microRNA-mediated translational repression in human cells subjected to stress. *Cell*, **125**, 1111–1124.
22. Vasudevan,S. and Steitz,J.A. (2007) AU-rich-element-mediated upregulation of translation by FXR1 and Argonaute 2. *Cell*, **128**, 1105–1118.
23. Nonhoff,U., Ralser,M., Welzel,F., Piccini,I., Balzereit,D., Yaspo,M.L., Lehrach,H. and Krobitsch,S. (2007) Ataxin-2 interacts with the DEAD/H-box RNA helicase DDX6 and interferes with P-bodies and stress granules. *Mol. Biol. Cell*, **18**, 1385–1396.
24. Chen,C., Ridzon,D.A., Broomer,A.J., Zhou,Z., Lee,D.H., Nguyen,J.T., Barbisin,M., Xu,N.L., Mahuvakar,V.R., Andersen,M.R. *et al*. (2005) Real-time quantification of microRNAs by stem-loop RT-PCR. *Nucleic Acids Res.*, **33**, e179.
25. Chen,Y. and Gorski,D.H. (2008) Regulation of angiogenesis through a microRNA (miR-130a) that down-regulates antiangiogenic homeobox genes GAX and HOXA5. *Blood*, **111**, 1217–1226.
26. Wang,G.L., Jiang,B.H., Rue,E.A. and Semenza,G.L. (1995) Hypoxia-inducible factor 1 is a basic-helix-loop-helix-PAS heterodimer regulated by cellular O2 tension. *Proc. Natl Acad. Sci. USA*, **92**, 5510–5514.
27. Fujioka,S., Sclabas,M.G., Schmidt,C., Niu,J., Frederick,A.W., Dong,G.Q., Abbruzzese,L.J., Evans,B.D., Baker,C. and Chiao,J.P. (2003) Inhibition of constitutive NF-κB activity by IκBαM suppresses tumorigenesis. *Oncogene*, **22**, 1365–1370.
28. Matsui,T., Hogetsu,K., Usukura,J., Sato,T., Kumasaka,T., Akao,Y. and Tanaka,N. (2006) Structural insight of human DEAD-box protein rck/p54 into its substrate recognition with conformational changes. *Genes Cells*, **11**, 439–452.
29. Lee,Y., Samaco,R.C., Gatchel,J.R., Thaller,C., Orr,H.T. and Zoghbi,H.Y. (2008) miR-19, miR-101 and miR-130 co-regulate ATXN1 levels to potentially modulate SCA1 pathogenesis. *Nat. Neurosci*, **11**, 1137–1139.
30. Kulshreshtha,R., Ferracin,M., Wojcik,S.E., Garzon,R., Alder,H., Agosto-Perez,F.J., Davuluri,R., Liu,C.G., Croce,C.M., Negrini,M. *et al*. (2007) A microRNA signature of hypoxia. *Mol. Cell. Biol.*, **27**, 1859–1867.

31. Fasanaro,P., D'Alessandra,Y., Di Stefano,V., Melchionna,R., Romani,S., Pompilio,G., Capogrossi,M.C. and Martelli,F. (2008) MicroRNA-210 modulates endothelial cell response to hypoxia and inhibits the receptor tyrosine kinase ligand Ephrin-A3. *J. Biol. Chem.*, **283**, 15878–15883.
32. Coller,J. and Parker,R. (2005) General translational repression by activators of mRNA decapping. *Cell*, **122**, 875–886.
33. Brengues,M., Teixeira,D. and Parker,R. (2005) Movement of eukaryotic mRNAs between polysomes and cytoplasmic processing bodies. *Science*, **310**, 486–489.
34. Bruno,I. and Wilkinson,M.F. (2006) P-bodies react to stress and nonsense. *Cell*, **125**, 1036–1038.
35. Serman,A., Le Roy,F., Aigueperse,C., Kress,M., Dautry,F. and Weil,D. (2007) GW body disassembly triggered by siRNAs independently of their silencing activity. *Nucleic Acids Res.*, **35**, 4715–4727.
36. Donker,R.B., Mouillet,J.F., Nelson,D.M. and Sadovsky,Y. (2007) The expression of Argonaute2 and related microRNA biogenesis proteins in normal and hypoxic trophoblasts. *Mol. Hum. Reprod.*, **13**, 273–279.
37. Diederichs,S. and Haber,D.A. (2007) Dual role for argonautes in microRNA processing and posttranscriptional regulation of microRNA expression. *Cell*, **131**, 1097–1108.
38. Lee,Y., Ahn,C., Han,J., Choi,H., Kim,J., Yim,J., Lee,J., Provost,P., Radmark,O., Kim,S. *et al.* (2003) The nuclear RNase III Drosha initiates microRNA processing. *Nature*, **425**, 415–419.